

Scattering from radiation-induced entangled states

Jin-Wook Jung, Kyungsun Na, and L. E. Reichl

Center for Complex Quantum Systems and Department of Physics, The University of Texas at Austin, Austin, Texas 78712, USA

(Received 22 December 2011; published 21 February 2012)

The scattering dynamics of a particle incident on a model system with three bound states in the presence of a localized radiation field is studied using Floquet scattering theory. An analytic expression for the Floquet S matrix is derived for the case of a radiation field containing two frequency components. The radiation field destabilizes and can entangle the bound states forming quasibound states that fundamentally alter the scattering dynamics of an incident particle.

DOI: [10.1103/PhysRevA.85.023420](https://doi.org/10.1103/PhysRevA.85.023420)

PACS number(s): 34.50.Rk, 32.80.-t, 03.65.Nk, 05.60.Gg

I. INTRODUCTION

Coherent time-periodic radiation interacting with matter can fundamentally change its dynamics. Energy is not conserved, but quasienergies (which are eigenphases of the Floquet states governing such systems) are conserved. The scattering of particles in the presence of coherent radiation can serve as a probe of the effect of the radiation on the internal dynamics of system. Radiation can destabilize bound states and entangle internal states in such a way that key features of the scatterer are radically altered.

The dynamics of a quantum system driven by a time-periodic field, with period T , is governed by a time-periodic Hamiltonian with period T . The solution to the Schrödinger equation for such processes is best obtained in terms of Floquet theory. Floquet theory allows the construction of Floquet scattering matrices that give the probability amplitude for transmission or reflection due to the emission or absorption of photons in the presence of the scattering potential and the driving field. Floquet scattering theory has been applied to a harmonically driven square barrier system [1], the scattering of an electron from an inverted Gaussian potential [2] in the presence of a single-mode radiation field, and the scattering of electrons from oscillating δ function potentials [3,4] for single-mode driving field. It has also been used to compute the conductance of electrons across oscillating barriers [5] and the conductance of electron pumps [6,7].

The systems described above, which are driven by a single-mode radiation field, conserve parity and generalized parity and exhibit a zero average current. Several authors have studied the dynamics of systems driven by two frequencies, one being an harmonic of the other (harmonic mixing) [8–10]. Rohling and Grossman [10] have shown that driving fields, with harmonic mixing and broken parity and generalized parity, give rise to a nonvanishing average currents.

The mixing of frequencies in a radiation field is a standard procedure for STIRAP (stimulated Raman adiabatic passage) based quantum control [11–14]. The use of Floquet theory to describe STIRAP processes was developed by Na and Reichl [15] and subsequently used by other authors on a variety of systems [16–19].

In this paper we obtain the Floquet scattering matrix for an exactly solvable open system, with bound states, that is driven by a single-mode radiation field and by a two-mode time-periodic driving field whose frequencies are chosen to resonant with the energy spacing of the bound states. We show

that an incident particle scatters from states that are radiation induced entangled superpositions of the bound states. The resulting scattering resonances in the transmission probability amplitudes occur at the quasienergies of the entangled states. We find that, although the radiation fundamentally changes the dynamics of the system, the incident particle can serve as a probe of this altered dynamics.

In subsequent sections we consider scattering from a square well potential that, in the absence of radiation, has three bound states. We assume that the potential well depth is periodically modulated by a space-dependent field. In Sec. II we introduce the model system and derive the Floquet eigenstates. In Sec. III we derive the Floquet scattering matrix and in Sec. IV we compute transmission probabilities for the single-frequency and two-frequency cases and show that scattering resonances occur at the quasienergies of the irradiated system. In Sec. V we make some concluding remarks.

II. THE SCATTERING SYSTEM

We consider a particle of mass μ in infinite space, but in the presence of the square well potential $V(x) = V_0 = -7.8$ for $-a \leq x \leq a$ and $V(x) = 0$ for $-\infty \leq x \leq -a$ and $a \leq x \leq \infty$ (all parameters are measured in atomic units). The values of V_0 and x were chosen to optimize the two-frequency resonances that we describe below. A sketch of the potential is given in Fig. 1. The energy spectrum consists of three bound states with energies $E_1 = -7.020$, $E_2 = -4.757$, and $E_3 = -1.397$ and a continuum of energies $0 \leq E \leq \infty$. The spacings between the bound state energies are $\Delta E_{32} = E_3 - E_2 = 3.360$ and $\Delta E_{21} = E_2 - E_1 = 2.263$.

We now add a two-mode time-periodic driving force to this system. The oscillating force is localized to the potential well. The Hamiltonian takes the form

$$H(t) = -\frac{\hbar^2}{2\mu} \frac{\partial^2}{\partial x^2} - |V_0| + V_1 x \cos(\omega_1 t) + V_2 x \cos(\omega_2 t) \quad (1)$$

for $-a \leq x \leq a$

and $H(t) = -\frac{\hbar^2}{2\mu} \frac{\partial^2}{\partial x^2}$ for $-\infty \leq x \leq -a$ and $a \leq x \leq \infty$. (In atomic units Planck's constant $\hbar = 1$.) We require that $\omega_1 = n_1 \omega$ and $\omega_2 = n_2 \omega$, where n_1 and n_2 are integers. The Hamiltonian is periodic in time with period $T = \frac{2\pi}{\omega}$. For the potential well depth $V_0 = -7.8$, a photon with frequency $\omega = 1.124$ resonates with energy levels E_2 and E_3 when $n_1 = 3$ and with energy levels E_1 and E_2 when $n_2 = 2$.

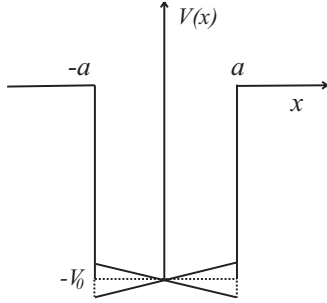


FIG. 1. Schematic diagram of the square-well potential with three bound state levels.

The Schrödinger equation can be written

$$i\hbar \frac{\partial \psi(x,t)}{\partial t} = -\frac{\hbar^2}{2\mu} \frac{\partial^2 \psi(x,t)}{\partial x^2} + [-|V_0| + V_1 x \cos(\omega_1 t) + V_2 x \cos(\omega_2 t)] \psi(x,t) \quad (2)$$

for $a \leq x \leq a$ and

$$i\hbar \frac{\partial \psi(x,t)}{\partial t} = -\frac{\hbar^2}{2\mu} \frac{\partial^2 \psi(x,t)}{\partial x^2} \quad (3)$$

for $\infty \leq x \leq -a$ and $a \leq x \leq \infty$. Because the Hamiltonian $H(t)$ for this system is time periodic, the Schrödinger equation has solutions which are eigenstates of the Floquet Hamiltonian $H_F(t) = H(t) - i\hbar \frac{\partial}{\partial t}$. The Floquet states can be written

$$\psi_\Omega(x,t) = e^{-i\Omega t/\hbar} \phi_\Omega(x,t), \quad (4)$$

where $\phi_\Omega(x,t)$ is periodic with the period $T = \frac{2\pi}{\omega}$ of the Hamiltonian $H(t)$ and the Floquet eigenvalues Ω have values that lie in the fundamental interval $0 \leq \Omega \leq \omega$. The states $\phi_\Omega(x,t)$ are eigenstates of the Floquet Hamiltonian $H_F(t)$ with eigenvalues $\hbar\Omega$. Any solution $\psi(x,t)$ of the Schrödinger equation can be expanded in terms of a spectral decomposition involving the Floquet eigenstates and eigenphases.

It is possible to obtain analytic solutions for the Floquet eigenstates in each spatial interval $-\infty \leq x \leq -a$, $-a \leq x \leq a$, and $a \leq x \leq \infty$. We can then require that the eigenstates and their slopes be continuous at the boundaries of these intervals to obtain Floquet eigenstates for the entire interval $-\infty \leq x \leq \infty$. Below we obtain these analytic solutions.

A. Region I ($-a \leq x \leq a$)

In region I ($-a \leq x \leq a$) we write the Floquet eigenstate in the form

$$\psi_\Omega^{(I)}(x,t) = e^{-i\Omega t/\hbar} \Phi(\xi,t) \chi(x,t), \quad (5)$$

$$\xi = x - \frac{V_1}{\mu\omega_1^2} \cos(\omega_1 t) - \frac{V_2}{\mu\omega_2^2} \cos(\omega_2 t), \quad (6)$$

and

$$\chi(x,t) = \exp \left\{ -i \left[\frac{V_1 x \sin(\omega_1 t)}{\hbar\omega_1} + \frac{V_2 x \sin(\omega_2 t)}{\hbar\omega_2} + f(t) \right] \right\}, \quad (7)$$

where

$$f(t) = -\frac{1}{2\mu\hbar} \left\{ \frac{V_1^2 \sin(2\omega_1 t)}{4\omega_1^3} + \frac{V_2^2 \sin(2\omega_2 t)}{4\omega_2^3} + \frac{V_1 V_2 \sin[(\omega_1 + \omega_2)t]}{\omega_1 \omega_2 (\omega_1 + \omega_2)} - \frac{V_1 V_2 \sin[(\omega_1 - \omega_2)t]}{\omega_1 \omega_2 (\omega_1 - \omega_2)} \right\}. \quad (8)$$

If we substitute Eq. (5) into Eq. (2) and note that

$$\frac{\partial \Phi}{\partial t} = \left(\frac{\partial \Phi}{\partial t} \right)_\xi + \left[\frac{V_1 \sin(\omega_1 t)}{\mu\omega_1} + \frac{V_2 \sin(\omega_2 t)}{\mu\omega_2} \right] \frac{\partial \Phi}{\partial \xi}, \quad (9)$$

we obtain

$$i\hbar \left(\frac{\partial \Phi}{\partial t} \right)_\xi = -\frac{\hbar^2}{2\mu} \frac{\partial^2 \Phi}{\partial \xi^2} + \left(\frac{V_1^2}{4\mu\omega_1^2} + \frac{V_2^2}{4\mu\omega_2^2} - |V_0| - \Omega \right) \Phi. \quad (10)$$

Now write $\Phi(\xi,t)$ in the form

$$\Phi(\xi,t) = \sum_{\ell=-\infty}^{\infty} e^{-i\ell\omega t} (\alpha_\ell e^{ik_\ell \xi} + \beta_\ell e^{-ik_\ell \xi}) \quad (11)$$

and substitute it into Eq. (10). This yields the dispersion relation

$$\frac{\hbar^2 k_\ell^2}{2\mu} = \Omega + \ell\hbar\omega + |V_0| - \frac{V_1^2}{4\mu\omega_1^2} - \frac{V_2^2}{4\mu\omega_2^2} \quad (12)$$

or

$$k_\ell = \sqrt{\frac{2\mu}{\hbar^2} \left(\Omega + \ell\hbar\omega + |V_0| - \frac{V_1^2}{4\mu\omega_1^2} - \frac{V_2^2}{4\mu\omega_2^2} \right)}. \quad (13)$$

If we now combine Eqs. (5), (6), (7), and (11), the Floquet eigenstate takes the form

$$\begin{aligned} \psi_\Omega^{(I)}(x,t) &= e^{-i\Omega t/\hbar} \exp \left\{ -i \left[\frac{V_1 x \sin(\omega_1 t)}{\hbar\omega_1} + \frac{V_2 x \sin(\omega_2 t)}{\hbar\omega_2} + f(t) \right] \right\} \\ &\times \sum_{\ell=-\ell_{\text{LB}}}^{\infty} e^{-i\ell\omega t} (\alpha_\ell e^{ik_\ell [x - \frac{V_1}{\mu\omega_1^2} \cos(\omega_1 t) - \frac{V_2}{\mu\omega_2^2} \cos(\omega_2 t)]} \\ &+ \beta_\ell e^{-ik_\ell [x - \frac{V_1}{\mu\omega_1^2} \cos(\omega_1 t) - \frac{V_2}{\mu\omega_2^2} \cos(\omega_2 t)]}). \end{aligned} \quad (14)$$

The lower bound ℓ_{LB} of the index ℓ is chosen to provide enough scattering channels to enable multiphoton transitions to the lowest energies available inside the potential well in the presence of radiation.

B. Region II ($-\infty \leq x \leq -a$)

In region II, for summation index $0 \leq \gamma \leq \infty$, the Floquet eigenstate (3) takes the form

$$\psi_\Omega^{(II)}(x,t) = e^{-i\Omega t/\hbar} \sum_{\gamma=0}^{\infty} e^{-i\gamma\omega t} \left(\frac{A_\gamma}{\sqrt{k_\gamma^0}} e^{ik_\gamma^0 x} + \frac{B_\gamma}{\sqrt{k_\gamma^0}} e^{-ik_\gamma^0 x} \right), \quad (15)$$

where the wave vector k_γ^0 is defined

$$k_\gamma^0 = \sqrt{\frac{2\mu}{\hbar^2} (\Omega + \gamma\hbar\omega)}, \quad (16)$$

A_γ is the probability amplitude of an incoming wave (from the left) in the γ th channel and B_γ is the probability amplitude of an outgoing wave (to the left) in the γ th channel. For summation index $-\ell_{\text{LB}} \leq \gamma < 0$, the Floquet eigenstate (3) takes the form

$$\psi_{\Omega}^{(\text{II})}(x,t) = e^{-i\Omega t/\hbar} \sum_{\gamma=-1}^{-\ell_{\text{LB}}} e^{-i\gamma\omega t} \left(\frac{E_\gamma}{\sqrt{\kappa_\gamma}} e^{+\kappa_\gamma x} \right), \quad (17)$$

where E_γ is the amplitude of states that tunnel into region II. The wave vector κ_γ is defined as

$$\kappa_\gamma = \sqrt{\frac{2\mu}{\hbar^2} (|\gamma|\hbar\omega - \Omega)}. \quad (18)$$

C. Region III ($a \leq x \leq \infty$)

In region III, for summation index $0 \leq \gamma \leq \infty$, the solution to the Schrödinger equation (3) takes the form

$$\psi_{\Omega}^{(\text{III})}(x,t) = e^{-i\Omega t/\hbar} \sum_{\gamma=0}^{\infty} e^{-i\gamma\omega t} \left(\frac{C_\gamma}{\sqrt{k_\gamma^0}} e^{ik_\gamma^0 x} + \frac{D_\gamma}{\sqrt{k_\gamma^0}} e^{-ik_\gamma^0 x} \right), \quad (19)$$

where D_γ is the probability amplitude of an incoming wave (from the right) in the γ th channel and C_γ is the probability amplitude of an outgoing wave (to the right) in the γ th channel. For summation index $-\ell_{\text{LB}} \leq \gamma < 0$, the Floquet eigenstate (3) takes the form

$$\psi_{\Omega}^{(\text{III})}(x,t) = e^{-i\Omega t/\hbar} \sum_{\gamma=-1}^{-\ell_{\text{LB}}} e^{-i\gamma\omega t} \left(\frac{F_\gamma}{\sqrt{\kappa_\gamma}} e^{-\kappa_\gamma x} \right), \quad (20)$$

where F_γ is the amplitude of states that tunnel into region III.

D. Boundary conditions

We can obtain a relation between the coefficients A_γ , B_γ , C_γ , D_γ , E_γ , F_γ , α_ℓ , and β_ℓ by equating the Floquet states and the slopes of the Floquet states at the interfaces $x = -a$ and $x = +a$.

1. Equate states at $x = +a$ and $x = -a$

If we set $\psi_{\Omega}^{(\text{I})}(+a,t) = \psi_{\Omega}^{(\text{III})}(+a,t)$, and then multiply both sides of the equation by $\frac{1}{2\pi} \int_0^{2\pi} d(\omega t) e^{iq\omega t}$, and integrate we obtain

$$\frac{C_q}{\sqrt{k_q^0}} e^{+ik_q^0 a} + \frac{D_q}{\sqrt{k_q^0}} e^{-ik_q^0 a} = \sum_{\ell=-\ell_{\text{LB}}}^{\infty} (M_{q,\ell} \alpha_\ell + N_{q,\ell} \beta_\ell) \quad (21)$$

for $q \geq 0$ and we obtain

$$\frac{F_q}{\sqrt{\kappa_q}} e^{-\kappa_q a} = \sum_{\ell=-\ell_{\text{LB}}}^{\infty} (M_{q,\ell} \alpha_\ell + N_{q,\ell} \beta_\ell) \quad (22)$$

for $q < 0$. The coefficients $M_{q,\ell}$ and $N_{q,\ell}$ are defined in Appendix A.

Similarly, if we set $\psi_{\Omega}^{(\text{I})}(-a,t) = \psi_{\Omega}^{(\text{II})}(-a,t)$, then multiply both sides of the equation by $\frac{1}{2\pi} \int_0^{2\pi} d(\omega t) e^{iq\omega t}$, and integrate we obtain

$$\frac{A_q}{\sqrt{k_q^0}} e^{-ik_q^0 a} + \frac{B_q}{\sqrt{k_q^0}} e^{ik_q^0 a} = \sum_{\ell=-\ell_{\text{LB}}}^{\infty} (R_{q,\ell} \alpha_\ell + S_{q,\ell} \beta_\ell) \quad (23)$$

for $q \geq 0$ and we obtain

$$\frac{E_q}{\sqrt{\kappa_q}} e^{-\kappa_q a} = \sum_{\ell=-\ell_{\text{LB}}}^{\infty} (R_{q,\ell} \alpha_\ell + S_{q,\ell} \beta_\ell) \quad (24)$$

for $q < 0$. The coefficients $R_{q,\ell}$ and $S_{q,\ell}$ are defined in Appendix A.

2. Equate slopes of states at $x = +a$ and $x = -a$

Let us now set $(\frac{d\psi_{\Omega}^{(\text{I})}(x,t)}{dx})_{x=+a} = (\frac{d\psi_{\Omega}^{(\text{III})}(x,t)}{dx})_{x=+a}$, multiply both sides of the equation by $\frac{1}{2\pi} \int_0^{2\pi} d(\omega t) e^{iq\omega t}$, and integrate. This gives

$$\sqrt{k_q^0} C_q e^{+ik_q^0 a} - \sqrt{k_q^0} D_q e^{-ik_q^0 a} = \sum_{\ell=-\ell_{\text{LB}}}^{\infty} (P_{q,\ell} \alpha_\ell + Q_{q,\ell} \beta_\ell) \quad (25)$$

for $q \geq 0$ and

$$-\sqrt{\kappa_q} F_q e^{-\kappa_q a} = \sum_{\ell=-\ell_{\text{LB}}}^{\infty} (i P_{q,\ell} \alpha_\ell + i Q_{q,\ell} \beta_\ell) \quad (26)$$

for $-\ell_{\text{LB}} \leq q \leq -1$. The coefficients $P_{q,\ell}$ and $Q_{q,\ell}$ are defined in Appendix A.

Similarly, if we set $(\frac{d\psi_{\Omega}^{(\text{I})}(x,t)}{dx})_{x=-a} = (\frac{d\psi_{\Omega}^{(\text{II})}(x,t)}{dx})_{x=-a}$, multiply both sides of the equation by $\frac{1}{2\pi} \int_0^{2\pi} d(\omega t) e^{iq\omega t}$, and integrate we obtain

$$\sqrt{k_q^0} A_q e^{-ik_q^0 a} - \sqrt{k_q^0} B_q e^{+ik_q^0 a} = \sum_{\ell=-\ell_{\text{LB}}}^{\infty} (U_{q,\ell} \alpha_\ell + V_{q,\ell} \beta_\ell) \quad (27)$$

for $q \geq 0$ and

$$\sqrt{\kappa_q} E_q e^{-\kappa_q a} = \sum_{\ell=-\ell_{\text{LB}}}^{\infty} (i U_{q,\ell} \alpha_\ell + i V_{q,\ell} \beta_\ell) \quad (28)$$

for $-\ell_{\text{LB}} \leq q \leq -1$. The coefficients $U_{q,\ell}$ and $V_{q,\ell}$ are defined in Appendix A.

III. DERIVATION OF THE FLOQUET S MATRIX

The Floquet S matrix (S_F matrix) relates incoming waves A_γ and D_γ to outgoing waves B_γ and C_γ . In order to obtain an expression for the S_F matrix, we must solve Eqs. (21)–(28). The first step is to write the equations as matrix equations. The indices q and ℓ have the range $-\ell_{\text{LB}} \leq q \leq \infty$. In practice we only need to keep a finite range of values for these indices. When the incident particle has very high energy, it will not be affected by the presence of the potential well and will transition through the scattering region without change in its trajectory. Thus we only need to retain a finite number $N + 1$ of positive

energy scattering channels. Below we will assume that the indices have the range $-\ell_{\text{LB}} \leq q \leq N$ and $-\ell_{\text{LB}} \leq \ell \leq N$, so that there are $N + 1$ propagating channels (each with width in energy equal to $\hbar\omega$) in the asymptotic regions. The value of the cutoff N is chosen such that further increase in N does not change the scattering properties of the system.

Let us now introduce the following column matrices for the propagating modes:

$$\begin{aligned} \mathcal{A} &= (A_N, \dots, A_0)^T, & \mathcal{B} &= (B_N, \dots, B_0)^T, \\ \mathcal{C} &= (C_N, \dots, C_0)^T, & \mathcal{D} &= (D_N, \dots, D_0)^T, \\ \boldsymbol{\alpha}_p &= (\alpha_N, \dots, \alpha_0)^T, & \boldsymbol{\beta}_p &= (\beta_N, \dots, \beta_0)^T, \end{aligned} \quad (29)$$

where T denotes transpose. Similarly for the evanescent modes we can write

$$\begin{aligned} \mathcal{E} &= (E_{-1}, \dots, E_{-M})^T, & \mathcal{F} &= (F_{-1}, \dots, F_{-M})^T, \\ \boldsymbol{\alpha}_e &= (\alpha_{-1}, \dots, \alpha_{-M})^T, & \boldsymbol{\beta}_e &= (\beta_{-1}, \dots, \beta_{-M})^T, \end{aligned} \quad (30)$$

where $M = \ell_{\text{LB}}$.

We define the square diagonal matrices of wave vectors as

$$(\eta_{ee})_{i,j} = \frac{1}{\sqrt{\kappa_i}} \delta_{i,j} \quad \text{and} \quad (\mathbf{K}_{pp}^{(\pm)})_{i,j} = e^{\pm i\sqrt{\kappa_i}a} \delta_{i,j}, \quad (31)$$

with $i = N, N-1, \dots, 1, 0$. Similarly,

$$(\eta_{pp})_{i,j} = \frac{1}{\sqrt{\kappa_i}} \delta_{i,j} \quad \text{and} \quad (\mathbf{K}_{pp}^{(\pm)})_{i,j} = e^{-\sqrt{\kappa_i}a} \delta_{i,j}, \quad (32)$$

with $i = -1, -2, \dots, -M$.

We also construct the following four matrices out of the coefficients $M_{q,\ell}$:

$$\mathbf{M}_{p,p} = \begin{pmatrix} M_{N,N} & \dots & M_{N,0} \\ \vdots & \ddots & \vdots \\ M_{0,N} & \dots & M_{0,0} \end{pmatrix}, \quad (33)$$

$$\mathbf{M}_{p,e} = \begin{pmatrix} M_{N,-1} & \dots & M_{N,-M} \\ \vdots & \ddots & \vdots \\ M_{0,-1} & \dots & M_{0,-M} \end{pmatrix},$$

$$\mathbf{M}_{e,p} = \begin{pmatrix} M_{-1,N} & \dots & M_{-1,0} \\ \vdots & \ddots & \vdots \\ M_{-M,N} & \dots & M_{-M,0} \end{pmatrix}, \quad (34)$$

$$\mathbf{M}_{e,e} = \begin{pmatrix} M_{-1,-1} & \dots & M_{-1,-M} \\ \vdots & \ddots & \vdots \\ M_{-M,-1} & \dots & M_{-M,-M} \end{pmatrix}.$$

We construct a similar set of four matrices for each of the remaining coefficients $N_{q,\ell}, P_{q,\ell}, Q_{q,\ell}, R_{q,\ell}, S_{q,\ell}, U_{q,\ell}$, and $V_{q,\ell}$.

In terms of the above matrices, Eqs. (21)–(24) can be written

$$\begin{aligned} \eta_{pp} \cdot \mathbf{K}_{pp}^{(-)} \cdot \mathcal{A} + \eta_{pp} \cdot \mathbf{K}_{pp}^{(+)} \cdot \mathcal{B} \\ = \mathbf{R}_{p,p} \cdot \boldsymbol{\alpha}_p + \mathbf{R}_{p,e} \cdot \boldsymbol{\alpha}_e + \mathbf{S}_{p,p} \cdot \boldsymbol{\beta}_p + \mathbf{S}_{p,e} \cdot \boldsymbol{\beta}_e, \end{aligned} \quad (35)$$

$$\eta_{ee} \cdot \mathbf{K}_{ee} \cdot \mathcal{E} = \mathbf{R}_{e,p} \cdot \boldsymbol{\alpha}_p + \mathbf{R}_{e,e} \cdot \boldsymbol{\alpha}_e + \mathbf{S}_{e,p} \cdot \boldsymbol{\beta}_p + \mathbf{S}_{e,e} \cdot \boldsymbol{\beta}_e, \quad (36)$$

$$\begin{aligned} \eta_{pp} \cdot \mathbf{K}_{pp}^{(+)} \cdot \mathcal{C} + \eta_{pp} \cdot \mathbf{K}_{pp}^{(-)} \cdot \mathcal{D} \\ = \mathbf{M}_{p,p} \cdot \boldsymbol{\alpha}_p + \mathbf{M}_{p,e} \cdot \boldsymbol{\alpha}_e + \mathbf{N}_{p,p} \cdot \boldsymbol{\beta}_p + \mathbf{N}_{p,e} \cdot \boldsymbol{\beta}_e, \end{aligned} \quad (37)$$

$$\eta_{ee} \cdot \mathbf{K}_{ee} \cdot \mathcal{F} = \mathbf{M}_{e,p} \cdot \boldsymbol{\alpha}_p + \mathbf{M}_{e,e} \cdot \boldsymbol{\alpha}_e + \mathbf{N}_{e,p} \cdot \boldsymbol{\beta}_p + \mathbf{N}_{e,e} \cdot \boldsymbol{\beta}_e, \quad (38)$$

respectively.

Equations (25)–(28) can be written

$$\begin{aligned} \eta_{pp}^{-1} \cdot \mathbf{K}_{pp}^{(-)} \cdot \mathcal{A} - \eta_{pp}^{-1} \cdot \mathbf{K}_{pp}^{(+)} \cdot \mathcal{B} \\ = \mathbf{U}_{p,p} \cdot \boldsymbol{\alpha}_p + \mathbf{U}_{p,e} \cdot \boldsymbol{\alpha}_e + \mathbf{V}_{p,p} \cdot \boldsymbol{\beta}_p + \mathbf{V}_{p,e} \cdot \boldsymbol{\beta}_e, \end{aligned} \quad (39)$$

$$-i\eta_{ee}^{-1} \cdot \mathbf{K}_{ee} \cdot \mathcal{E} = \mathbf{U}_{e,p} \cdot \boldsymbol{\alpha}_p + \mathbf{U}_{e,e} \cdot \boldsymbol{\alpha}_e + \mathbf{V}_{e,p} \cdot \boldsymbol{\beta}_p + \mathbf{V}_{e,e} \cdot \boldsymbol{\beta}_e, \quad (40)$$

$$\begin{aligned} \eta_{pp}^{-1} \cdot \mathbf{K}_{pp}^{(+)} \cdot \mathcal{C} - \eta_{pp}^{-1} \cdot \mathbf{K}_{pp}^{(-)} \cdot \mathcal{D} \\ = \mathbf{P}_{p,p} \cdot \boldsymbol{\alpha}_p + \mathbf{P}_{p,e} \cdot \boldsymbol{\alpha}_e + \mathbf{Q}_{p,p} \cdot \boldsymbol{\beta}_p + \mathbf{Q}_{p,e} \cdot \boldsymbol{\beta}_e, \end{aligned} \quad (41)$$

$$i\eta_{ee}^{-1} \cdot \mathbf{K}_{ee} \cdot \mathcal{F} = \mathbf{P}_{e,p} \cdot \boldsymbol{\alpha}_p + \mathbf{P}_{e,e} \cdot \boldsymbol{\alpha}_e + \mathbf{Q}_{e,p} \cdot \boldsymbol{\beta}_p + \mathbf{Q}_{e,e} \cdot \boldsymbol{\beta}_e, \quad (42)$$

respectively.

After considerable matrix algebra, we can solve these equations to obtain

$$\begin{pmatrix} \mathcal{B} \\ \mathcal{C} \end{pmatrix} = \mathbf{S}_F \begin{pmatrix} \mathcal{A} \\ \mathcal{D} \end{pmatrix}, \quad (43)$$

where

$$\mathbf{S}_F = \begin{pmatrix} \mathbf{r}' & \mathbf{t} \\ \mathbf{t}' & \mathbf{r} \end{pmatrix} \quad (44)$$

is the $(2N+2) \times (2N+2)$ Floquet scattering matrix. The submatrices \mathbf{t} and \mathbf{t}' are $(N+1) \times (N+1)$ matrices of transmission probability amplitudes and \mathbf{r} and \mathbf{r}' are $(N+1) \times (N+1)$ matrices of reflection probability amplitudes. For example, the matrix \mathbf{t} has the structure

$$\mathbf{t} = \begin{pmatrix} t_{N,N} & \dots & t_{N,0} \\ \vdots & \ddots & \vdots \\ t_{0,N} & \dots & t_{0,0} \end{pmatrix}, \quad (45)$$

where $t_{n,n'}$ is the probability amplitude for transmission from the n th Floquet scattering channel to the n' th Floquet scattering channel.

IV. TRANSMISSION PROBABILITIES

We can now calculate the transmission probability for a particle of mass $\mu = 1$ (in atomic units) that scatters from the oscillating potential region ($-a \leq x \leq a$). We assume that the particle, asymptotically, has energy E . To determine the relevant scattering channel in the Floquet matrix, we note that $E = \Omega + n\hbar\omega$. The value of integer n that satisfies this equation determines the incident scattering channel in the Floquet scattering matrix. The theory that we developed in previous sections, allows us to compute transmission probabilities for scattering in the presence of either single-mode or two-mode radiation. We will consider both types of scattering process below.

In Appendix B we have derived the Floquet eigenphases for a bounded three-level model (TLM) consisting of the three bound energy states driven by the radiation field. The TLM

contains the effect of the radiation on the bound states in the potential well without influence from the continuum. The three Floquet states for the TLM have their support primarily on a single bound state (one bound state for each Floquet state) when the radiation is out of resonance. When radiation is resonant with pairs of bound states, the bound states become entangled. The TLM describes the essential physics inside the potential well when radiation is present. When a pair of bound states is in resonance with the radiation field, one Floquet state will consist primarily of the nonresonant bound state

and the other two Floquet states will consist of symmetric and antisymmetric superpositions of the two resonant bound states. These superposition states are entangled pairs of bound states. As we shall show, it is the entangled bound states that scatter the incident particle

For scattering in the presence of single-mode radiation, we consider first (case I) a radiation field with frequency $\omega_1 = 3.372$ which resonates with energy levels E_2 and E_3 , and then (case II) a radiation field with frequency $\omega_2 = 2.248$ which resonates with energy levels E_1 and E_2 . In each case, the radiation entangles the two resonant bound states and the incident particle scatters from the entangled states. We will also consider the case (case III) in which the incident particle scatters from the potential region with two-mode radiation. We will compare the transmission resonances to Floquet eigenvalues for TLM in Appendix B.

A. Case I: Single-mode scattering for $n_1 = 1, n_2 = 0, V_2 = 0,$ and $\omega_1 = 3\omega = 3.372$

We compute the transmission probability $|t_{0,0}|^2$ for an incident particle with energy $0 \leq E \leq \omega_1$ (so $E = \Omega$). This gives the probability that the particle, which is incident in the $n = 0$ channel, will be transmitted past the scattering potential in channel $n = 0$. The radiation field with frequency $\omega_1 = 3.372$ has been chosen to resonate with bound states E_2

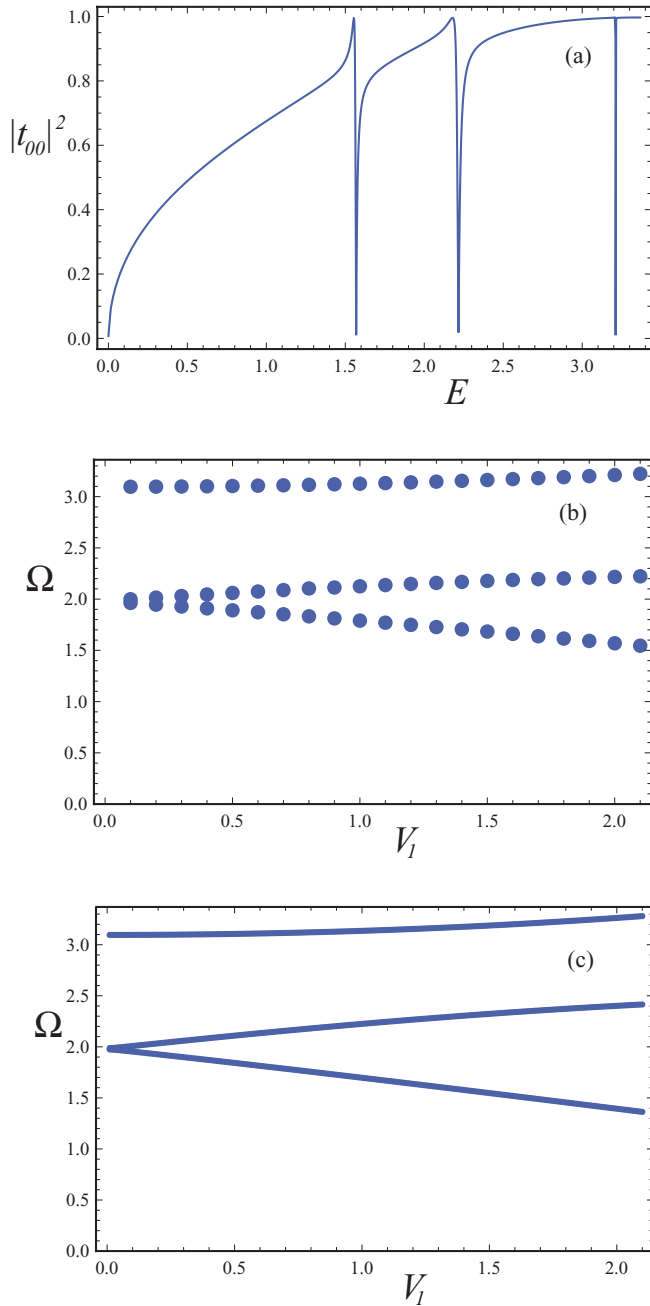


FIG. 2. (Color online) (a) Plot of transmission probability $|t_{0,0}|^2$ as a function of energy of the incident particle for $V_1 = 2.0, V_2 = 0,$ and $\omega_1 = 3.372$. (b) The transmission zeros of $|t_{0,0}|^2$ as a function of V_1 . (c) The Floquet eigenphases for the TLM as a function of V_1 for $V_2 = 0$ and $\omega_1 = 3.372$. All quantities in atomic units.

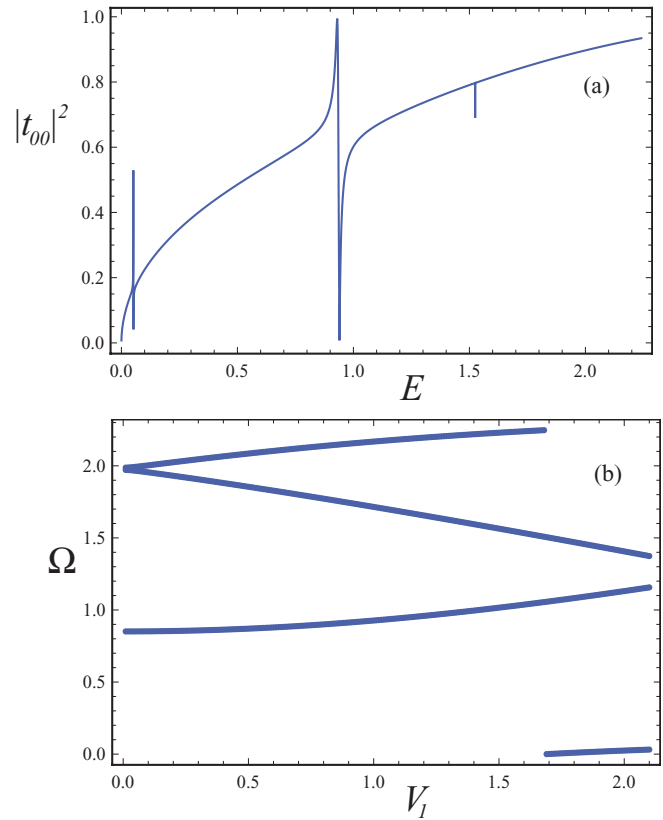


FIG. 3. (Color online) (a) Plot of transmission probability $|t_{0,0}|^2$ as a function of energy of the incident particle for $V_1 = 0, V_2 = 2.0,$ and $\omega_2 = 2.248$. (b) The Floquet eigenphases for the TLM as a function of V_2 for $V_1 = 0$ and $\omega_2 = 2.248$. All quantities in atomic units.

and E_3 . The transmission probability, as a function of incident energy $E = \Omega$, is shown in Fig. 2(a) for $V_1 = 2.0$. There are three energies, $E = 1.569$, $E = 2.217$, and $E = 3.211$, at which the transmission probability goes to zero. In Fig. 2(b) we

plot the location of the transmission probability zeros of $|t_{0,0}|^2$ as a function of radiation field amplitude V_1 . In Fig. 2(c) we plot the Floquet eigenvalues for the TLM discussed in Appendix B. We see that the location of the transmission probability zeros

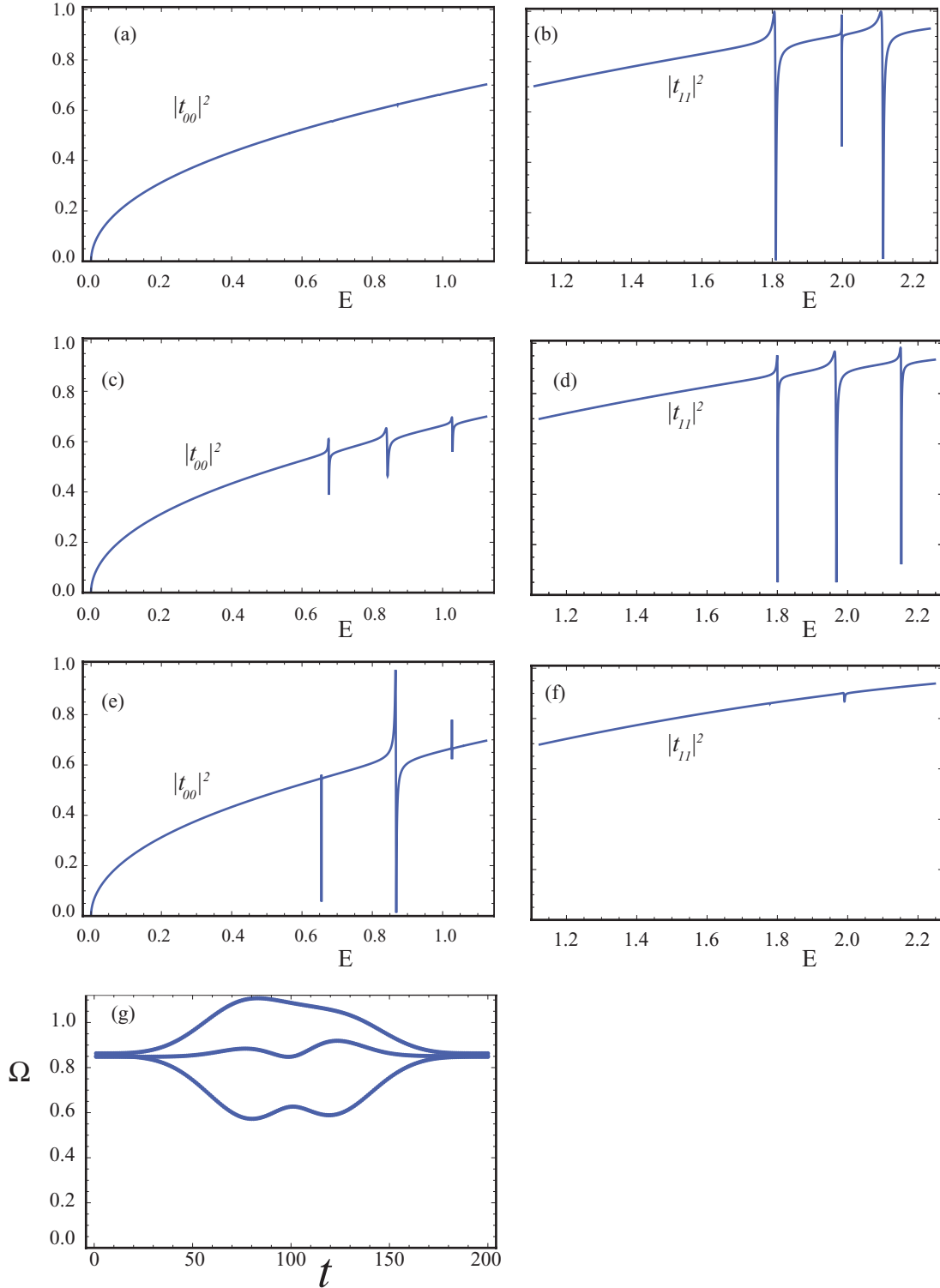


FIG. 4. (Color online) Transmission probabilities for (a) $|t_{0,0}|^2$ with ($V_1 = 0.08, V_2 = 0.90$), (b) $|t_{1,1}|^2$ with ($V_1 = 0.08, V_2 = 0.90$), (c) $|t_{0,0}|^2$ with ($V_1 = 0.67, V_2 = 0.67$), (d) $|t_{1,1}|^2$ with ($V_1 = 0.67, V_2 = 0.67$), (e) $|t_{0,0}|^2$ with ($V_1 = 0.90, V_2 = 0.08$), and (f) $|t_{1,1}|^2$ with ($V_1 = 0.90, V_2 = 0.08$). (g) Plot of Floquet eigenphases of the TLM as radiation amplitudes are turned on and the off as described in Appendix B. All quantities in atomic units.

is almost identical to the Floquet eigenvalues for the TLM, namely $\Omega_{B,2} = 1.394$, $\Omega_{B,3} = 2.401$, and $\Omega_{B,1} = 3.262$. The incident particle is resonating with the Floquet states created by the matter-field interaction inside the potential well. As the radiation amplitude $V_1 \rightarrow 0$, the Floquet eigenphase $\Omega_1 \rightarrow E_1 + 3\omega_1 = 3.06$ (modulus 3.372), and other two Floquet eigenphases for the TLM become degenerate and take on values $\Omega_2 \rightarrow E_2 + 2\omega_1 = 1.984$ (modulus 3.372) and $\Omega_3 \rightarrow E_3 + \omega_1 = 1.972$ (modulus 3.372). This degeneracy is lifted as the radiation field amplitude is increased. In the limit $V_1 \rightarrow 0$, two of the transmission zeros become degenerate as well, indicating that the incident particle is resonating with the entangle states inside the potential well.

B. Case II: Single-mode scattering for $n_1 = 0$, $n_2 = 1$, $V_1 = 0$, and $\omega_2 = 2\omega = 2.248$

We compute the transmission probability $|t_{0,0}|^2$ for an incident particle with energy $0 \leq E \leq \omega_2$ (so $E = \Omega$). We consider a single-mode radiation field with frequency $\omega_2 = 2.248$ and external field strength $V_2 = 2.0$ ($V_1 = 0.0$). The radiation field resonates with bound states E_1 and E_2 . The transmission probability, as a function of incident energy (in the zeroth channel), is shown in Fig. 3(a). There are three energies, $E = 0.052$, $E = 0.94$, and $E = 1.525$, at which the transmission probability goes to zero. In Fig. 3(b) we plot the Floquet eigenvalues for the TLM (Appendix B) for $V_2 = 2$. Again we see that the location of the transmission probability zeros is almost identical to the Floquet eigenvalues of the bounded system $\Omega_{B,2} = 0.025$, $\Omega_{B,3} = 1.131$, and $\Omega_{B,1} = 1.406$. The incident particle is resonating with the Floquet states inside the potential well created by the matter-field interaction.

C. Case III: Two-mode scattering for $\omega_1 = 3\omega$, $\omega_2 = 2\omega$, $V_j = V_0 e^{-m(t-\tau_j)^2}$ ($j = 1, 2$), $\tau_1 < \tau_2$, and $\omega = 1.124$

We compute the transmission probability for the case when the system is driven by two frequencies $\omega_1 = 3\omega = 3.372$ and $\omega_2 = 2\omega = 2.248$, where $\omega = 1.124$. The transmission probabilities $|t_{0,0}|^2$ ($|t_{1,1}|^2$) for a particle with incident energy in the interval $0 \leq E \leq \omega$ ($\omega \leq E \leq 2\omega$) are shown in Fig. 4. Transmission resonances for external field strengths ($V_1 = 0.90$, $V_2 = 0.08$) are given in Figs. 4(a) and 4(b), transmission resonances for ($V_1 = 0.67$, $V_2 = 0.67$) are given in Figs. 4(c) and 4(d), and transmission resonances for ($V_1 = 0.08$, $V_2 = 0.90$) are given in Figs. 4(e) and 4(f). These plots give the probability that the particle, which is incident in the $n = 0$ ($n = 1$) channel, will be transmitted past the scattering potential into channel $n = 0$ ($n = 1$).

Scattering resonances occur in both incident channels. When the particle is incident in the zeroth channel the resonances are weak for the cases with ($V_1 = 0.90$, $V_2 = 0.08$) and ($V_1 = 0.67$, $V_2 = 0.67$). The transmission probability does not go to zero. When the particle is incident in the first channel, the resonances are strong in terms of transmission zeros. However, when ($V_1 = 0.08$, $V_2 = 0.90$) transmission resonances are strong for a particle incident in the zeroth channel but weak for first channel scattering. In Fig. 4(c) the resonances occur at energies $E = 0.675$, $E = 0.843$, and

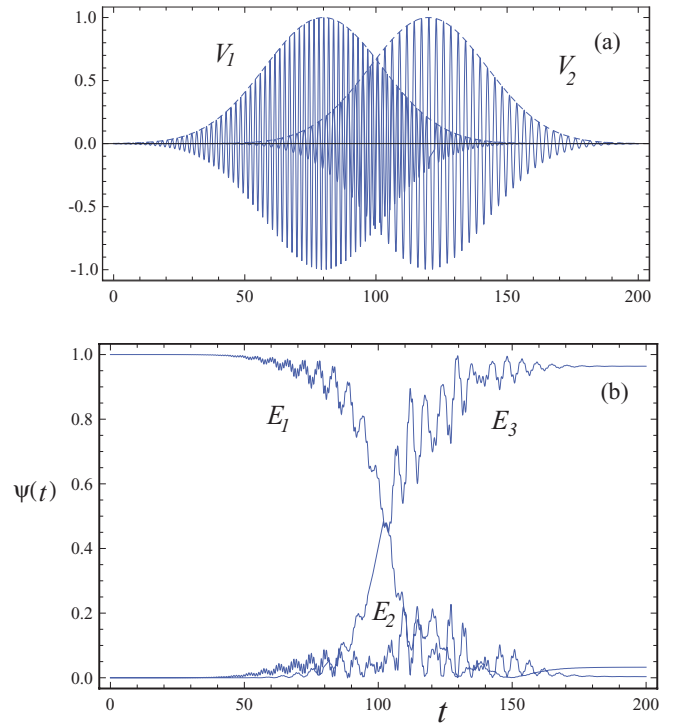


FIG. 5. (Color online) (a) Plot of time dependence of radiation “pulses” applied to the TLM. (b) Evolution of probability in the state $|\psi(t)\rangle$ of the TLM as the radiation pulses are turned on and then off. All quantities in atomic units.

$E = 1.028$ for the zeroth channel and in Fig. 4(d) they occur at $E = 0.675 + \omega$, $E = 0.843 + \omega$, and $E = 1.028 + \omega$.

In Fig. 4(g) we show the variation in the three Floquet eigenvalues of the TLM (Appendix B) as the amplitudes of the radiation fields are turned on and off in a Gaussian manner [see Fig. 5(a)]. The location of the scattering resonances shown in Figs. 4(b)–4(e) coincide with the Floquet eigenvalues of the TLM. We see that, again, the incident particle scatters from the Floquet states created in the potential well by the radiation field. These values agree well with the Floquet energies in Fig. 4(b) at 0.626, 0.848, and 1.087.

V. CONCLUSION

We have derived the Floquet scattering matrix for a particle incident on a potential well whose depth oscillates in time by a localized multimode radiation field. We have shown that the particle can act as a probe of the Floquet eigenstates of the oscillating system. Internal states, such as bound states for the radiation free system, are destabilized by the radiation and can be entangled by it. These entangled states form quasibound states that resonate with the incident particle and dramatically affect its scattering behavior.

ACKNOWLEDGMENT

The authors wish to thank the Robert A. Welch Foundation (Grant No. F-1051) for support of this work.

APPENDIX A

Introduce the function

$$I_{q,\ell}(s_1, s_2, s_3, s_4) = \frac{1}{2\pi} \int_0^{2\pi} d\theta e^{i(q-\ell)\theta} e^{s_1 i k_\ell a} e^{s_2 i a g(\theta)} e^{s_3 i f(\theta)} e^{s_4 i k_\ell h(\theta)}, \quad (\text{A1})$$

where $\theta = \omega t$, $s_i = \pm 1$ (for $i = 1, 2, 3, 4$), and

$$\begin{aligned} g(\theta) &= \frac{V_1 \sin(n_1 \theta)}{\hbar n_1 \omega} + \frac{V_2 \sin(n_2 \theta)}{\hbar n_2 \omega}, \\ h(\theta) &= \frac{V_1 \cos(n_1 \theta)}{\mu n_1^2 \omega^2} + \frac{V_2 \cos(n_2 \theta)}{\mu n_2^2 \omega^2}, \\ f(\theta) &= -\frac{1}{2\mu\hbar} \left\{ \frac{V_1^2 \sin(2n_1 \theta)}{4n_1^3 \omega^3} + \frac{V_2^2 \sin(2n_2 \theta)}{4n_2^3 \omega^3} \right. \\ &\quad \left. + \frac{V_1 V_2 \sin[(n_1 + n_2)\theta]}{n_1 n_2 (n_1 + n_2) \omega^3} - \frac{V_1 V_2 \sin[(n_1 - n_2)\theta]}{n_1 n_2 (n_1 - n_2) \omega^3} \right\}. \end{aligned} \quad (\text{A2})$$

Then

$$\begin{aligned} M_{q,\ell} &= I_{q,\ell}(+, -, -, -), & N_{q,\ell} &= I_{q,\ell}(-, -, -, +), \\ R_{q,\ell} &= I_{q,\ell}(-, +, -, -), & S_{q,\ell} &= I_{q,\ell}(+, +, -, +). \end{aligned} \quad (\text{A3})$$

Similarly, introduce the function

$$J_{q,\ell} = \frac{1}{2\pi} \int_0^{2\pi} d\theta e^{i(q-\ell)\theta} [s_0 k_\ell - g(\theta)] \times e^{s_1 i k_\ell a} e^{s_2 i a g(\theta)} e^{s_3 i f(\theta)} e^{s_4 i k_\ell h(\theta)}. \quad (\text{A4})$$

Then

$$\begin{aligned} P_{q,\ell} &= J_{q,\ell}(+, +, -, -, -), \\ Q_{q,\ell} &= J_{q,\ell}(-, -, -, -, +), \\ U_{q,\ell} &= J_{q,\ell}(+, -, +, -, -), \\ \text{and } V_{q,\ell} &= J_{q,\ell}(-, +, +, -, +). \end{aligned} \quad (\text{A5})$$

APPENDIX B: THREE-LEVEL MODEL (TLM)

In the presence of radiation, the three bound states form a basis for computing the three Floquet states inside the potential well. In this Appendix we neglect the continuum and compute the evolution of the system governed by Eq. (2), using the bound state energy eigenstates $|E_1\rangle$, $|E_2\rangle$, and $|E_3\rangle$ as the basis. Then $|\psi(t)\rangle = \sum_{n=1}^3 \psi_n(t) |E_n\rangle$ and the Schrödinger equation takes the form of a 3×3 matrix equation

$$\begin{aligned} \frac{d\psi_n(t)}{dt} &= -i E_n \psi_n(t) - i [V_1 \cos(\omega_1 t) + V_2 \cos(\omega_2 t)] \\ &\quad \times \sum_{m=1}^3 \langle E_n | x | E_m \rangle \psi_m(t), \end{aligned} \quad (\text{B1})$$

where $\psi_n(t) = \langle E_n | \psi(t) \rangle$ is the probability amplitude to find the system in the n th energy level ($n = 1, 2, 3$) at time t . The solutions to these equations can be written in the form

$$\psi_n(t) = \sum_{\alpha=1}^3 A_{n,\alpha} e^{-i\Omega_{B,\alpha} t} \langle E_n | \phi_\alpha(t) \rangle, \quad (\text{B2})$$

where $\Omega_{B,\alpha}$ is the Floquet eigenphase, $A_{n,\alpha} = \langle \phi_\alpha(0) | \psi(0) \rangle$, and $|\phi_\alpha(t)\rangle$ is the α th ($\alpha = 1, 2, 3$) Floquet eigenstate. The state of the system at time $t = T$ is given by

$$\psi_n(T) = \sum_{\alpha=1}^3 \sum_{m=1}^3 e^{-i\Omega_{B,\alpha} T} \langle E_n | \phi_\alpha(0) \rangle \langle \phi_\alpha(0) | E_m \rangle \psi_m(0). \quad (\text{B3})$$

The Floquet evolution matrix is then given by

$$U_{n,m}(T) = \sum_{\alpha=1}^3 e^{-i\Omega_{B,\alpha} T} \langle E_n | \phi_\alpha(0) \rangle \langle \phi_\alpha(0) | E_m \rangle \quad (\text{B4})$$

and is a unitary matrix. The matrix $U_{n,m}(T)$ evolves the system forward in time by one period of the driving field. The n th column of $U_{n,m}(T)$ is obtained by integrating Eq. (B1) with initial condition $\psi_m(0) = 1$ for $m = n$ and $\psi_m(0) = 0$ for $m \neq n$. The α th eigenvalue of $U_{n,m}(T)$ is $e^{-i\Omega_{B,\alpha} T}$ so $\Omega_{B,\alpha} = i \ln(e^{-i\Omega_{B,\alpha} T})/T$. Below we consider three different cases for the driving field.

1. Case I: Single-mode driving for $n_1 = 1$, $n_2 = 0$, $V_2 = 0$, and $\omega_1 = 3.372$

The single-mode driving field resonates with energy levels E_2 and E_3 . A plot of the Floquet eigenvalues $\Omega_{B,\alpha}$ (defined modulus $\omega_1 = 3.372$) as a function of the amplitude of the driving V_1 is given in Fig. 2(c). In the limit $V_1 \rightarrow 0$, $\Omega_{B,1} = E_1 + 3\omega_1 = -7.02 + 3 \times 3.372 = 3.096$. The curves $\Omega_{B,2}$ and $\Omega_{B,3}$ in the limit $V_1 \rightarrow 0$ become degenerate and are entangled combinations of the energy levels $|E_2\rangle$ and $|E_3\rangle$. Note that $\Omega_{B,2} = E_2 + 2\omega_1 = -4.76 + 2 \times 3.372 = 1.984$ and $\Omega_{B,3} = E_3 + \omega_1 = -1.4 + 1 \times 3.372 = 1.972$.

2. Case II: Single-mode driving for $n_1 = 0$, $n_2 = 1$, $V_1 = 0$, and $\omega_2 = 2.248$

The single-mode driving field resonates with energy levels E_1 and E_2 . A plot of the Floquet eigenvalues $\Omega_{B,\alpha}$ (defined modulus $\omega_2 = 2.248$) as a function of the amplitude of the driving V_2 is given in Fig. 3(b). In the limit $V_2 \rightarrow 0$, $\Omega_{B,3} = E_3 + 1\omega_2 = -1.4 + 1 \times 2.248 = 0.848$. The curves $\Omega_{B,1}$ and $\Omega_{B,2}$ in the limit $V_2 \rightarrow 0$ become degenerate and are entangled combinations of the energy levels $|E_1\rangle$ and $|E_2\rangle$. Note that $\Omega_{B,1} = E_1 + 4\omega_2 = -7.02 + 4 \times 2.248 = 1.984$ and $\Omega_{B,2} = E_2 + \omega_2 = -4.76 + 3 \times 2.248 = 1.972$.

3. Case III: Two-mode driving for $\omega_1 = 3\omega$, $\omega_2 = 2\omega$, $V_j = V_0 e^{-m(t-\tau_j)^2}$ (with $j = 1, 2$ and $\tau_1 < \tau_2$), and $\omega = 1.124$

We drive the system with two sequential and slightly overlapping Gaussian shaped adiabatic pulses. The pulses [shown in Fig. 5(a)] can be considered adiabatic if the period of their carrier frequencies is much shorter than the duration of the pulses. In Eq. (B1) we replace V_1 and V_2 by $V_1(t) = V_0 e^{-m(t-\tau_1)^2}$ and $V_2(t) = V_0 e^{-m(t-\tau_2)^2}$, respectively, where τ_j ($\tau_1 < \tau_2$) are the times when the pulses are at their maximum values. The first (second) pulse, with carrier frequency 2ω (3ω), resonates (approximately) with levels E_2 and E_3 (E_1 and E_2).

Since the pulses are adiabatic, we can follow the evolution of the Floquet eigenphases and eigenstates as the pulses interact with the three-level system [15–19]. We divide the pulses into time windows and compute the Floquet eigenvalues and eigenstates for each time window with $V_1(t)$ and $V_2(t)$ held fixed to their value at the center of the time window. Floquet eigenstates of neighboring time windows will be approximately orthogonal, so we can continuously follow the changes in the Floquet eigenvalues during the time that the pulses act on the system. The Floquet eigenvalues (defined modulus $\omega = 1.124$) are shown in Fig. 4(d) as a function of time.

Near $t = 0$, the Floquet eigenstate $|\phi_1\rangle$ is predominantly composed of the energy state $|E_1\rangle$ with the Floquet eigenphase $\Omega_{B,1} = E_1 + 7\omega = -7.02 + 7 \times 1.124 = 0.86(\text{modulus } 1.124)$. The eigenstates $|\phi_2\rangle$ and $|\phi_3\rangle$ are symmetric and antisymmetric, respectively, superpositions of states $|E_2\rangle$ and $|E_3\rangle$ with the Floquet eigenphases $\Omega_{B,2} = E_2 + 5\omega = -4.76 + 5 \times 1.124 =$

$0.86(\text{modulus } 1.124)$ and $\Omega_{B,3} = E_3 + 2\omega = -1.4 + 2 \times 1.124 = 0.843(\text{modulus } 1.124)$, respectively. As time approaches $t = 100$, where there is a three-way avoided crossing among the three Floquet eigenphases, the eigenstates change their character. After the three-way avoided crossing, $|\phi_1\rangle$ has exchanged its support from the energy state $|E_1\rangle$ to support from energy state $|E_3\rangle$, and $|\phi_2\rangle$ and $|\phi_3\rangle$ have changed their character from superpositions of $|E_2\rangle \pm |E_3\rangle$ to superpositions of $|E_1\rangle \pm |E_2\rangle$.

If we start the system in energy state $|E_1\rangle$, so that $|\psi(-\infty)\rangle = |E_1\rangle$, then after the pulses have passed, the system will have been transferred to energy state $|E_3\rangle$ with almost 100% certainty. This process is shown in Fig. 5(b), where we solve the Schrödinger equation (B1) for $|\psi(t)\rangle$ and show the values of $|\langle E_n|\psi(t)\rangle|^2$ as the pulses pass through the system. Because of the avoided crossing near $t = 100$, the entire population gets shifted from state $|E_1\rangle$ to state $|E_3\rangle$ in a traditional STIRAP process [11–19].

-
- [1] W. Li and L. E. Reichl, *Phys. Rev. B* **60**, 15732 (1999).
 - [2] A. Emmanouilidou and L. E. Reichl, *Phys. Rev. A* **65**, 033405 (2002).
 - [3] D. F. Martinez and L. E. Reichl, *Phys. Rev. B* **64**, 245315 (2001).
 - [4] D. F. Martinez, L. E. Reichl, and G. A. Luna-Acosta, *Phys. Rev. B* **66**, 174306 (2002).
 - [5] W. Li and L. E. Reichl, *Phys. Rev. B* **62**, 8269 (2000).
 - [6] M. Moskalets and M. Buttiker, *Phys. Rev. B* **66**, 205320 (2002).
 - [7] S. W. Kim, *Phys. Rev. B* **66**, 235304 (2002).
 - [8] I. Goychuk and P. Hanggi, *Europhys. Lett.* **43**, 503 (1998).
 - [9] S. Kohler, J. Lehmann, and P. Hanggi, *Phys. Rep.* **406**, 379 (2005).
 - [10] N. Rohling and F. Grossmann, *Phys. Rev. B* **83**, 205310 (2011).
 - [11] J. Oreg, F. T. Hioe, and J. H. Eberly, *Phys. Rev. A* **29**, 690 (1984).
 - [12] U. Gaubatz, P. Rudecki, S. Schieman, and K. Bergmann, *J. Chem. Phys.* **92**, 5363 (1990).
 - [13] A. K. Bergmann, H. Theuer, and B. W. Shore, *Rev. Mod. Phys.* **70**, 1003 (1998).
 - [14] C. Y. Ye, V. A. Sautenkov, Y. V. Rostovtsev, and M. O. Scully, *Opt. Lett.* **28**, 2213 (2003).
 - [15] K. Na and L. E. Reichl, *Phys. Rev. A* **70**, 063405 (2004); **72**, 013402 (2005).
 - [16] K. Na, L. E. Reichl, and C. Jung, *J. Chem. Phys.* **125**, 034301 (2006).
 - [17] B. P. Holder and L. E. Reichl, *Phys. Rev. A* **76**, 013420 (2007).
 - [18] A. Roy and L. E. Reichl, *Phys. Rev. A* **77**, 033418 (2008).
 - [19] A. Roy and L. E. Reichl, *Physica E* **42**, 1627 (2010).